Electronic Supplementary Information

A Chemical-bond Driven Edge Reconstruction of Sb Nanoribbons and Their Thermoelectric Properties from First-principles Calculations

Jin-Ni Shen,[‡a,b] Yi Fang,[‡a] Zi-Xiong Lin,[c] Tian-Zhu Xie,[a] Yong-Fan Zhang,[d] Li-Ming, Wu*[e]

a. *College of Materials Science and Engineering, Fuzhou University, Fujian 350108, People's Republic of China.*

b. *Key Laboratory of Eco-materials Advanced Technology (Fuzhou University), Fujian Province University, Fuzhou 350002, China*

c. *Key Laboratory of Design and Assembly of Functional nanostructures, Fujian Institute of Research on the Structure of Matter, Chinese Academy of Sciences, Fuzhou, Fujian 350002, People's Republic of China*

d. *Department of Chemistry, Fuzhou University, Fujian 350108, People's Republic of China*

e. *Department of Chemistry, Beijing Normal University, Beijing, People's Republic of China.*

‡These authors contributed equally to this work.

†Electronic Supplementary Information (ESI) available: [details of any supplementary information available should be included here]. See DOI: 10.1039/x0xx00000x

Table S1. Binding energies (BEs), formation energies (FEs) and edge energies (EEs), band gaps (Gap) and ZT for ZSNRs-recon with symmetrically arranged motifs and staggered arranged motifs, respectively. The former ones have slightly higher formation energies and smaller TE performance than staggered ones, and also have nearly width-independent band gaps.

NRs	BE	FE*	EE	Gap	ZT	
	eV/atom	eV/atom	eV/Å	eV	n-type	p-type
symmetrically arranged motifs						
ZSNR-recon-4	-3.761	0.127	0.124	1.24	0.67	0.84
ZSNR-recon-6	-3.801	0.085	0.125	1.19	0.60	0.98
ZSNR-recon-8	-3.823	0.064	0.124	1.25	0.56	0.77
ZSNR-recon-10	-3.840	0.051	0.123	1.23	0.67	0.51
staggered arranged motifs						
ZSNR-recon-4	-3.759	0.125	0.122	1.15	0.72	1.22
ZSNR-recon-6	-3.800	0.084	0.124	1.22	0.63	0.97
ZSNR-recon-8	-3.822	0.063	0.123	1.24	0.55	0.74
ZSNR-recon-10	-3.835	0.050	0.123	1.24	0.60	0.65

*FE = (E(SNR) – N×E(Sb))/N

where E(SNR), E(Sbatom) and E(Sb) are the total energies of SNR per supercell, and that of a monolayer Sb nanosheet per atom, respectively. N is the number of Sb atoms in a supercell

Table S2. Fitted Parameters in the Morse Potential for the SNRs-recon, r_c = 6.0 Å.[a]

NRs	D_e eV	a 1/Å	r_0 Å
ASNR-recon-7	0.556	0.019	3.469
ASNR-recon-8	1.053	1.418	3.181
ASNR-recon-9	1.018	1.463	3.169
ASNR-recon-10	1.043	1.421	3.190
ASNR-recon-11	1.161	1.247	3.278
ASNR-recon-12	1.047	1.413	3.203
ASNR-recon-13	1.113	1.293	3.261
ASNR-recon-14	0.999	1.496	3.172
ASNR-recon-15	1.001	1.527	3.162
ASNR-recon-16	0.971	1.612	3.138
ASNR-recon-17	1.065	1.400	3.134
ZSNR-recon-4	0.795	1.315	3.189
ZSNR-recon-5	0.752	1.898	3.026
ZSNR-recon-6	0.692	1.980	3.097
ZSNR-recon-7	0.731	1.958	3.123
ZSNR-recon-8	0.869	1.492	3.163
ZSNR-recon-9	0.891	1.943	3.034
ZSNR-recon-10	0.921	1.774	3.107
ZSNR-recon-11	0.795	1.942	3.038

[a] Here D_e is the depth of the potential well, in eV, a is the measure of bond elasticity, r_0 is the equilibrium bond distance, and r_c is the cutoff distance .

We studied SbNRs with saturated hydrogen atoms and found that the edge reconstructed ones have lower binding energy than H-terminated ones as shown in Fig. S1. It is clearing that the binding energies of H-terminated ASNR decreases as dimer-layer (or width). Interesting, ANSR-unrecon-17 have a closer BE valve compared with its reconstructed one. As the dimer layer increases, the proportion of edge atoms decreases drastically, and the influence of edge atoms on the system also decreases. As a result, the BE can be gradually reduced and closed the reconstructed one at about -3.84 eV/atom. A similar behavior is also observed in ZSNR, where the BE of H-terminated lowers from -2.41 to -3.00 eV/atom and is higher than reconstructed. ZSNRs have 8 edge atoms in a unit cell, while ASNRs have 4. The role of H-terminated atoms in ZSNRs cannot be ignored. All systems are also investigated by both spin unpolarized and polarized. The magnetic moment is ~1 μB per edge Sb atom. The spin-polarized have higher BE value than the non-magnetic ones either AM or FM configurations. Hence, only the spin unpolarized results are presented in the discussion.

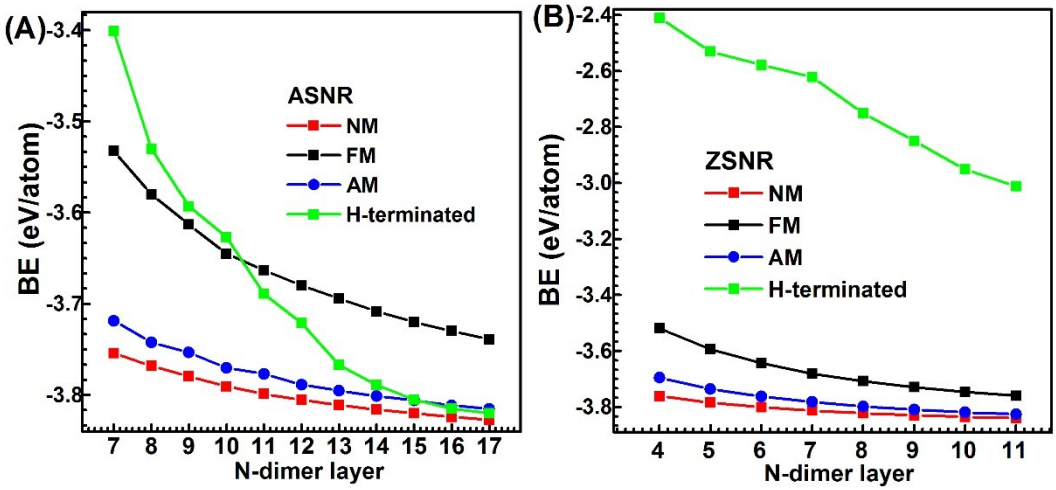

Fig. S1. The binding energies of SbNRs-recon with spin unpolarized (nonmagnetic, NM) and polarized (ferromagnetic, FM and antimagnetic, AM), and SbNRs-unrecon with H-terminated: (A) ASNR and (B) ZSNR.

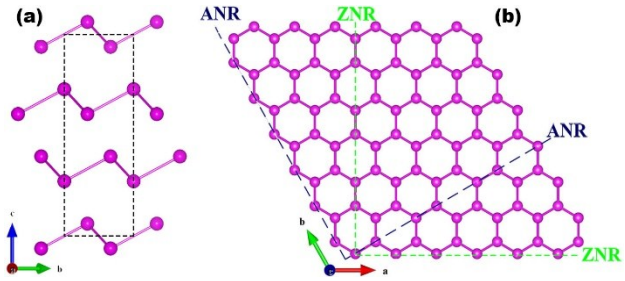

Fig. S2. (a) Bulk Sb structure, blank rectangles represent the 1×1×1 unit cell; (b) The top of view of Sb Nanosheet, the blank lines represent the cutting path of armchair nanoribbons, while the green lines are zigzag nanoribbons.

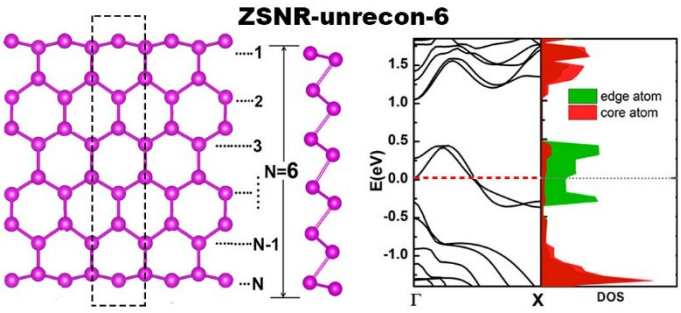

Fig. S3. The band structures of ZSNRs-unrecon-6.

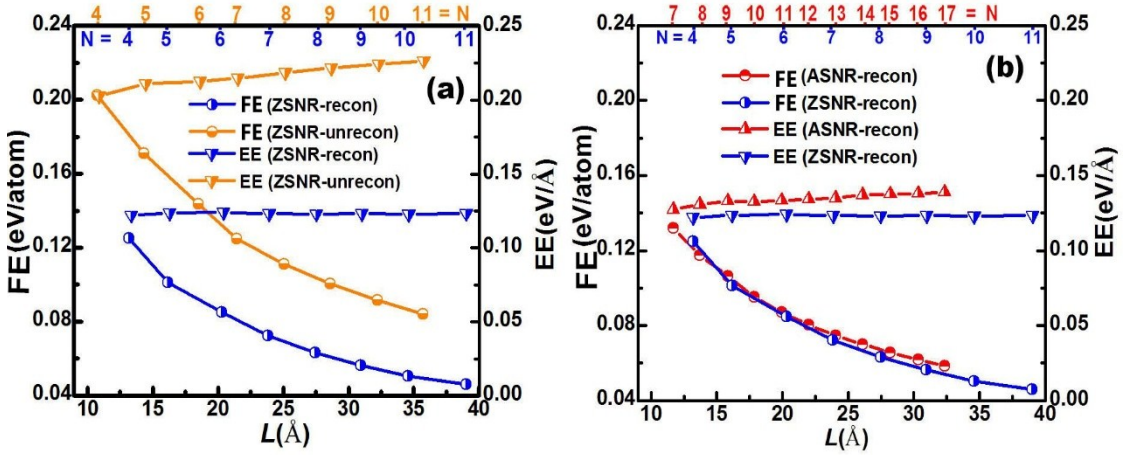

Fig. S4. The calculated formation energies (FEs, in the unit of eV per Sb atom) and edge energies (EEs, in the unit of eV per Å) as a function of the ribbon width of: (a) the unreconstructed (orange) and reconstructed (blue) ZSNRs; (b) the reconstructed ASNRs (red) and ZSNRs (blue). The top numbers are represented the number of dimer lines or zigzag chains.

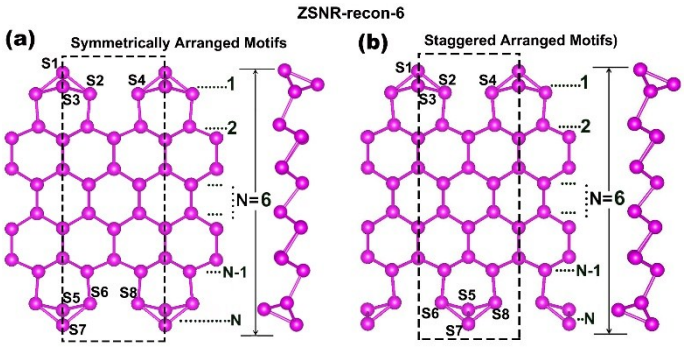

Fig. S5. Top and side of ZSNR-recon-6 with (a) symmetrically arranged motifs; (b) staggered arranged motifs. Blank rectangles represent the 1×1×1 unit cell adopted in calculation.

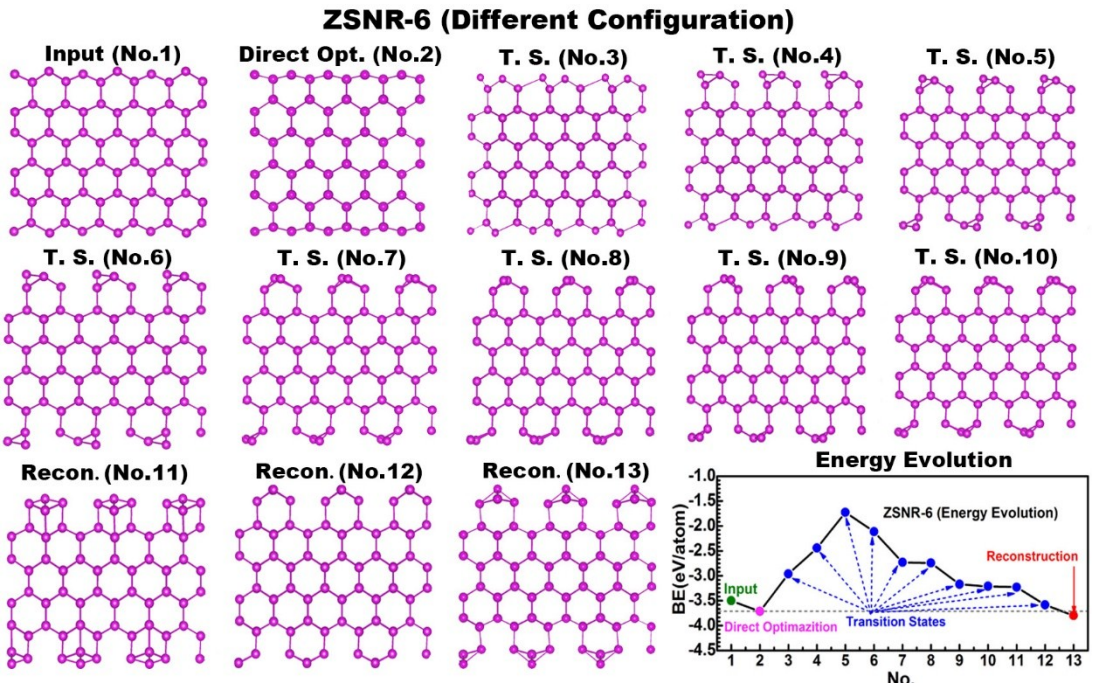

Fig. S6. Binding energy (BE) of ZSNR-6 for different edge constructed. Input means the initial structure without any optimization; Direct Opt, direct optimization structure from initial one; T. S., transition states with partial reconfiguration of edge atoms; Recon, edge atoms reconstructed by hands and then relaxed fully.

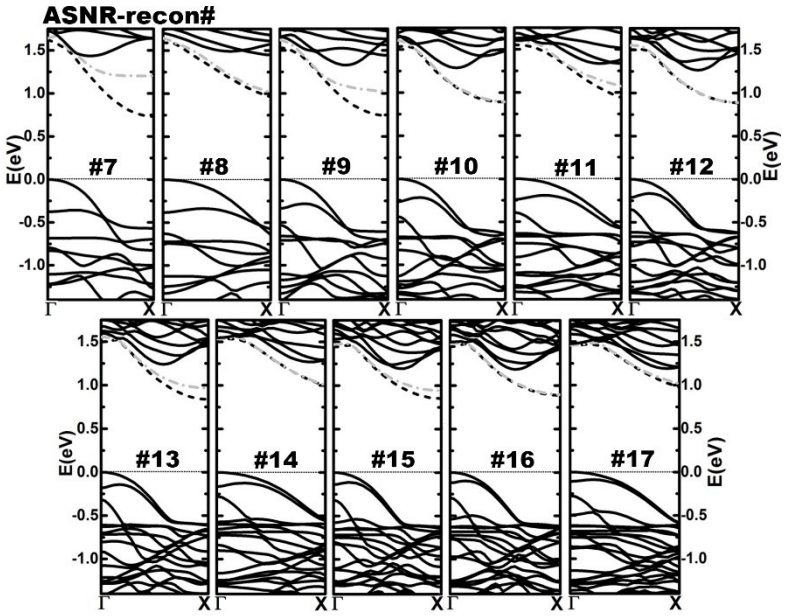

Fig. S7. The band structures of ASNRs-recon. The bank dash, gray dot dash lines respectively represent the bottom conduction band, the second bottom conduction band.

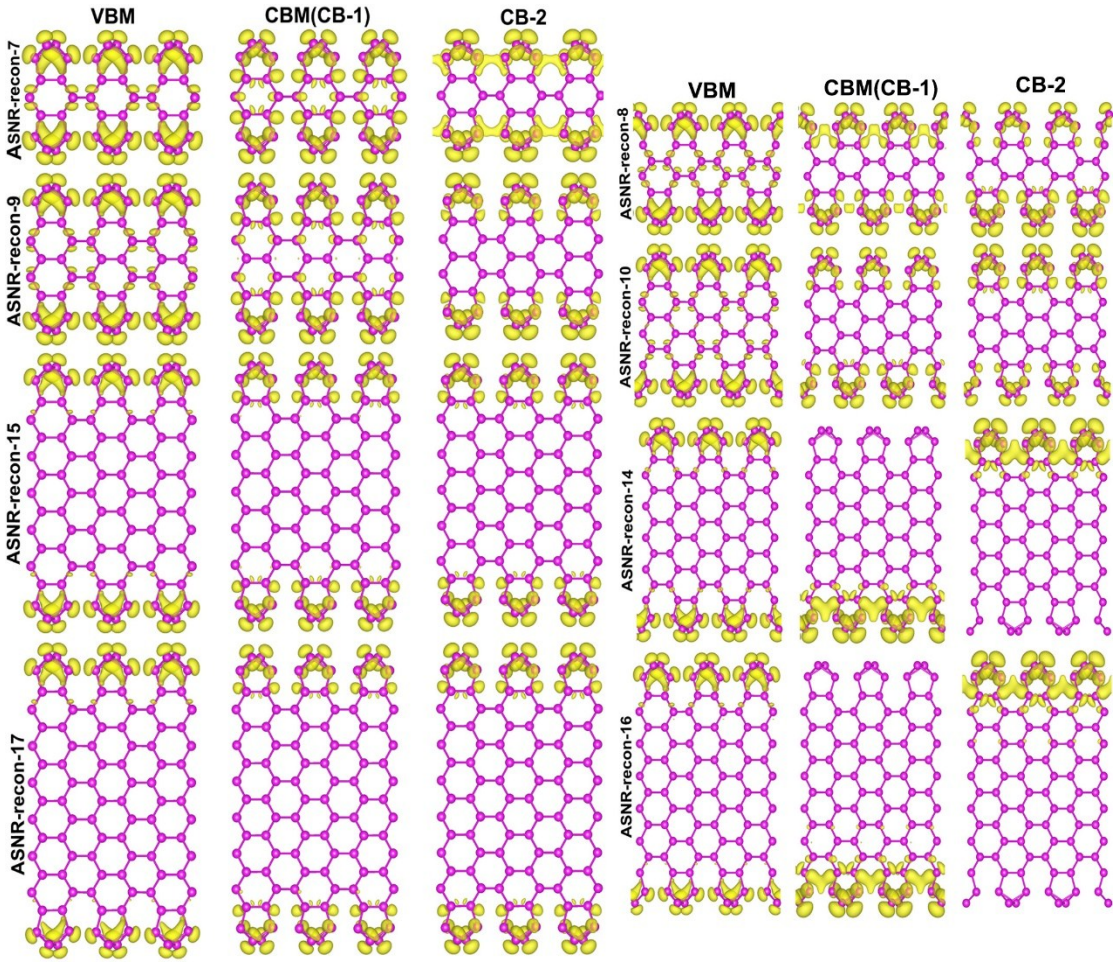

Fig. S8. Decomposed charge densities of ASNRs-recon.

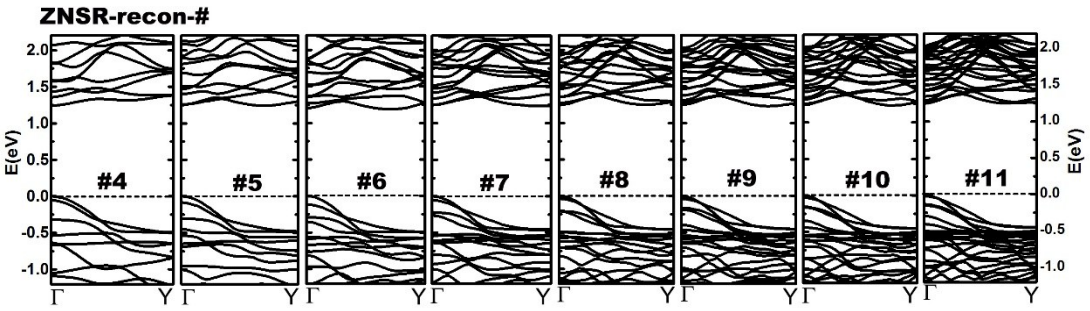

Fig. S9. The band structures of ZSNRs-recon.

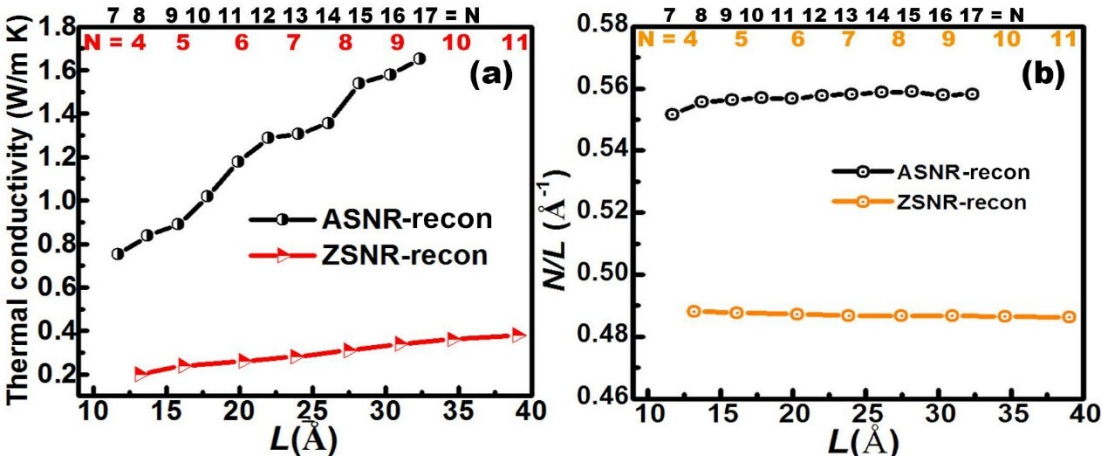

Fig. S10. (a) The lattice thermal conductivity of SNRs calculated using Green-Kubo equations. Circles and triangles respectively represent ASNRs-recon and ZSNRs-recon respectively; (b) the density of atoms per length (N/L) in a dimer lines or zigzag chains. The top numbers are represented the number of dimer lines or zigzag chains.

Fitting of the relaxation time

The accurate evaluation of the relaxation time depends on the detailed scattering mechanism. Here we use a simple approach in which the relaxation time τ is estimated by fitting the experimentally measured electrical conductivity or resistivity. Unfortunately, such experimental data is not available for Sb Nanoribbons, and as an alternative, we use the corresponding bulk value. This is a reliable approximation since Sb Nanoribbon has very similar covalent bonding compared to that of the bulk structure, as confirmed by our calculated charge densities. Such an approach has been widely used in previous works modeling the electronic transport of nanoscale systems.[1-4] The fitted relaxation time in the temperature region from 77 to 277 K[5] is summarized in Fig S8. As the electron scattering is more frequent at high temperatures, we find that the relaxation time τ decreases with increasing temperature and can befitted as

$$\tau \times 10^{13} = 1.19 + 29.11 \times \exp(-T/56.23) \quad (1)$$

We assume that the relaxation time of a Sb nanoribbons is independent of carrier concentration since it does not vary much around the Fermi level. The relaxation time is 1.3×10^{-13} s at 300 K from the fitted results.

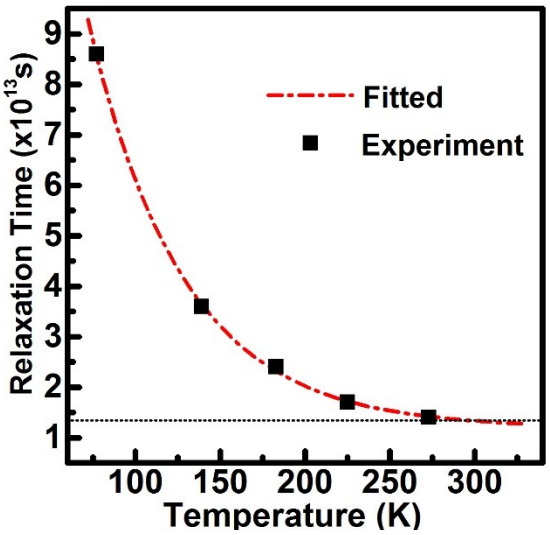

Fig. S11. Fitted Relaxation Time at Different Temperatures.

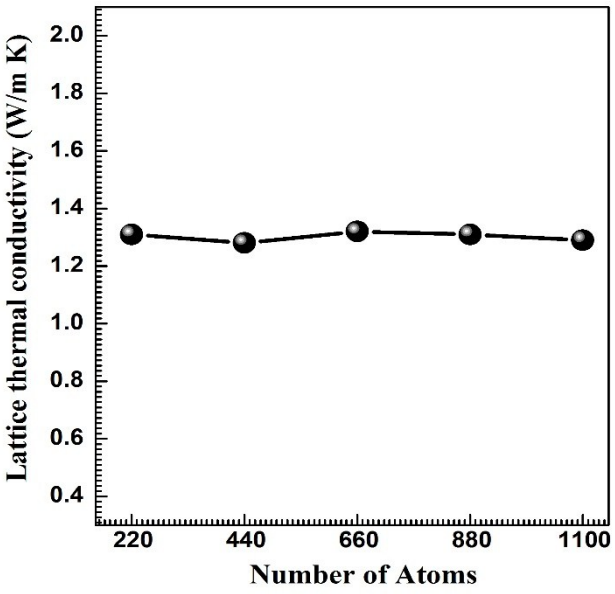

Fig. S12. Calculated thermal conductivity of ASNR-recon-12 as a function of N, where N is the number of atoms in the simulation cell. The temperature of simulation is 300 K.

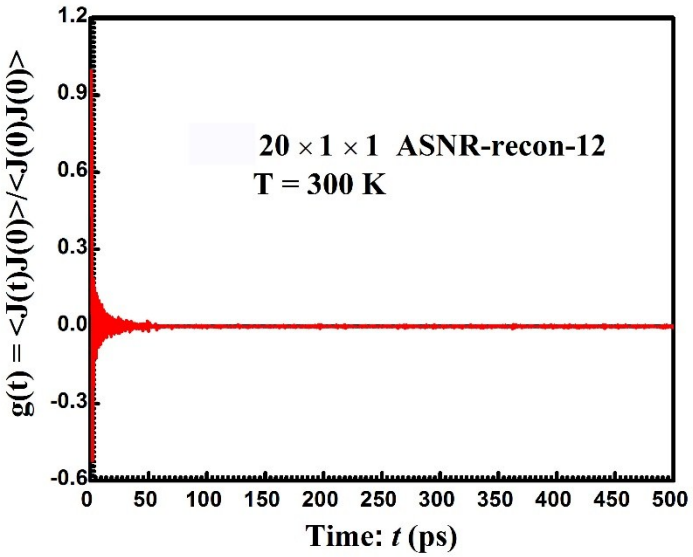

Fig. S13. The normalized time-dependent correlation function $g(\tau)$ = <J(τ)J(0)>/<J(0)J(0)> vs t at room temperature of ASNR-recon-12 system containing a total of 440 atoms.

Refrence

(1) Vo, T. T. M.; Williamson, A. J. Lordi, V.; Galli, G. *Nano Lett.* 2008, **8**, 1111.

(2) Chen, X.; Wang Y. C.; Ma, Y. M. *J. Phys. Chem. C* 2010, **114**, 9096.

(3) Chen, X.; Wang, Z.; Ma, Y. M. *J. Phys. Chem. C* 2011, **115**, 20696.

(4) Cheng, L.; Liu, H.; Tan, X.; Zhang, J.; Wei, J.; Lv, H.; Shi, J.; Tang, X. *J. Phys. Chem. C* 2014, **118**, 904.

(5) Öktu, O. Saunders, G. A. *Proc. Phys. Soc.* 1967, **91**, 156.